

1  
2  
3  
4  
5  
6  
7  
8 **Improvement of Soil Respiration Parameterization in a Dynamic Global Vegetation**  
9 **Model and Its Impact on the Simulation of Terrestrial Carbon Fluxes**  
10  
11  
12

13  
14 Dongmin Kim<sup>1</sup>, Myong-In Lee<sup>1\*</sup>, and Eunkyo Seo<sup>1</sup>  
15

16 <sup>1</sup>School of Urban and Environmental Engineering, UNIST, Ulsan, Korea  
17  
18  
19  
20  
21  
22  
23  
24  
25  
26  
27  
28  
29  
30  
31  
32  
33

34 January 12, 2017  
35  
36  
37  
38  
39  
40  
41

42 -----  
43 Corresponding author address: Dr. Myong-In Lee  
44 School of Urban and Environmental Engineering  
45 Ulsan National Institute of Science and Technology,  
46 100 Banyeon-ri, Ulju-gun, Ulsan 689-798, Korea  
47 Email: [milee@unist.ac.kr](mailto:milee@unist.ac.kr)

## Abstract

Soil decomposition is one of the critical processes in maintaining terrestrial ecosystem and global carbon cycle. Soil respiration ( $R_s$ ) sensitivity to temperature so called the  $Q_{10}$  value required for parameterizing soil decomposition process is assumed to be a constant in conventional numerical models, while it is not so in the realistic case with spatiotemporal heterogeneity. This study develops a new parameterization method for determining  $Q_{10}$  by considering the soil respiration dependence on soil temperature and moisture obtained by multiple regression. This study further investigates the impacts of the new parameterization on the global terrestrial carbon flux. Our results show that non-uniform spatial distribution of  $Q_{10}$  tends to represent the dependence of the soil respiration process on heterogeneous surface vegetation type compared with the control simulation using a uniform  $Q_{10}$ . Moreover, it tends to improve the simulation of the observed relationship between soil respiration and soil temperature and moisture, particularly over cold and dry regions. The homogenous distribution of decomposition processes tended to change carbon assimilation over land. This change of ununiformed spatial distribution of carbon assimilation improves the simulation of gross primary production (GPP) by enhanced nutrient assimilation from soil to vegetation. It leads to a more realistic spatial distribution of GPP, particularly over high latitudes (60–80 N) where the original model has a significant underestimation bias. In addition, overestimation bias of GPP in the tropics and the midlatitudes is significantly reduced. Improvement in the spatial distribution of GPP leads to a substantial reduction of global mean bias of GPP from + 9.11 to + 1.68 GtC yr<sup>-1</sup> compared with the FLUXNET-MTE observation data. The modified  $Q_{10}$  parameterization is possible to improve the simulation of global carbon cycle in CMIP5 ESMs which are based on the soil decomposition with constant  $Q_{10}$  values.



## 1. Introduction

Vegetated land surface affects climate (Foley et al., 1998; Sellers et al., 1986) and is affected by climate significantly (Bonan, 2008), forming complex interactions and feedback loops critical to climate change (Friedlingstein et al., 2006; Gregory et al., 2009). The land surface components of Earth System Models (ESMs) have evolved from only representing biophysical processes (i.e., hydrology and energy cycling) to including biogeochemical processes, such as dynamic vegetation change and carbon and nutrient cycles driven by ecosystems (Oleson et al., 2013; Sitch et al., 2003; Wang et al., 2010). The carbon balance of terrestrial ecosystems is the result of the balance between carbon uptake and loss by plants and soil respiration (Beer et al., 2010; Malhi et al., 1999; Le Que re et al., 2009, 2014; Luyssaert et al., 2007; Trumbore, 2006). Which terrestrial ecosystems act dominantly as sinks or sources has been a subject of considerable interest in studies of future climate change. Precise evaluation for each sink and source component and their responses to environmental factors are essential for reliable projection of future climate change by ESMs.

Future climate change projection by various ESMs driven by identical anthropogenic emissions is diverse and highly uncertain in the prediction of atmospheric CO<sub>2</sub> concentration (Friedlingstein et al., 2006, 2014; Hoffman et al., 2013). Many previous studies (Friedlingstein et al., 2006; Hoffman et al., 2013; Anav et al., 2013; Aroa et al., 2013; Friedlingstein et al., 2014) suggested that the uncertainty of CO<sub>2</sub> concentrations simulated by the emission-driven ESMs should be attributed to the carbon cycle over land rather than over ocean. In particular, One of the main causes seems to be related to our poor knowledge on carbon exchange by soil, leading to significant diversity among the model simulations (Todd-Brown et al., 2013). Diversity in the parameterization of photosynthesis at the leaf level is small compared with that of the soil decomposition process in contemporary ESMs with an interactive carbon cycle. Microbial decomposition of soil organic matter produces a major carbon flux from the

subsurface biosphere. Many studies investigated the response of soil respiration ( $R_s$ ) under global warming, and most of them suggested the warming would accelerate the release of  $CO_2$  from soil in future (Cox et al., 2000; Dufresne et al., 2002; Friedlingstein et al., 2003; Suseela et al., 2012). However, the amplitude of soil decomposition process has not been quantified through direct field measurements in the global domain, and highly uncertain, mostly due to the lack of observation data and poor estimates of it indirectly from soil temperature (Sussela et al., 2012). Moreover, Luo et al., (2016) suggested that the optimal parameter calibration in the model parameterization based on observation is needed to improve the soil carbon projection in ESMs. The reduction of uncertainty in the soil biogeochemical process remains a challenge for the ESM modeling community.

Soil respiration ( $R_s$ ) is considered a significant source of  $CO_2$  from terrestrial ecosystems. Recent studies suggest that  $CO_2$  emission change by soil should be largely driven by surface temperature change (Bond-Lamberty and Thomson, 2010). At global, regional and local scales, soil temperature and soil moisture are considered the most important abiotic parameters determining  $R_s$  (Kutsch et al., 2009). Empirical response functions based on heterogeneous field measurements are commonly used to derive annual estimates of  $R_s$  (Tang et al., 2005).

The sensitivity of soil respiration ( $R_s$ ) to temperature, the so-called  $Q_{10}$  value, is required for parameterizing the soil decomposition process. Whether this value is a global constant or variable in space is still under debate and the conclusions from the previous studies are diverse, which reflect our limited understanding to the soil respiration process. For example, Mahech et al. (2010) suggested that the  $Q_{10}$  value is independent of mean annual temperature and biomes. Karhu et al. (2014) also mentioned that the  $Q_{10}$  is approximately a global constant about 1.4 in the high latitude regions in the northern hemisphere. Another studies, on the other hand, suggested that  $Q_{10}$  may vary in space (Zhou et al., 2009; Xu and Qi, 2001; Qi et al., 2002). Belay-Tedla et al. (2009) suggested that warming-induced changes in plant growth and

community structure can considerably influence the quality and quantity of substrates which in turn regulates the responses of soil respiratory C release to rising temperature. All the abiotic and biotic factors such as soil temperature (Lloyd and Taylor, 1994; Kirschbaum, 1995; Luo et al., 2001), moisture (Davidson et al., 1998; Reichstein et al., 2002; Hui and Luo, 2004), and soil organic matter (Taylor et al., 1989; Liski et al., 1999; Wan and Luo, 2003) are heterogeneous, showing substantial spatial variation globally. Accordingly, estimated  $Q_{10}$  from measured soil respiration possibly varies at various geographic locations (Xu and Qi, 2001).

Based on the aforementioned studies, Zhao et al. (2009) developed an inverse model to retrieve the global pattern of heterogeneous  $Q_{10}$  values by assimilating soil organic carbon data with a process-based biogeochemical model. They suggested that spatial distribution of  $Q_{10}$  values changes according to vegetation type, with an increasing tendency as latitude increases. The impact on the estimation of carbon release due to  $Q_{10}$  variation in space is a significant change of approximately 25–40 % compared with the use of a constant  $Q_{10}$  value in Zhao et al. (2009). This result suggests that the determination of  $Q_{10}$  value is very important for the simulation of carbon-climate feedback and future climate change. However, most advanced ESMs participated in Coupled Model Intercomparison Project Phase 5 (CMIP5) still use a globally-constant  $Q_{10}$  value in the dynamic global vegetation models (Anav et al. 2013; Todd-Brown et al. 2013). In this case, the sensitivity of subsurface carbon flux under global warming condition would not be reflected in the model simulation.

Motivated by the above, this study developed a new parameterization method for determining  $Q_{10}$  by considering the dependence of soil respiration on soil temperature and moisture, the relationship of which was obtained from multiple regression with those two predictors. The variation of dominant vegetation type for the given area was also considered when determining  $Q_{10}$ . Community Land Model version 4 (CLM4) has the parameterization of the interactive carbon and nitrogen (C-N) cycle for the dynamic vegetation model, which was

used to derive realistic spatial distributions of  $Q_{10}$ . Moreover, the realistic soil carbon decomposition processes affect not only  $R_s$  but also primary production by improving nitrogen assimilation from soil to vegetation. This study further investigates the impacts of the new parameterization on the global carbon cycle.

Section 2 describes the observation and modeling data used in this study and the modeling method used to obtain the distribution of  $Q_{10}$ . Section 3 provides the results from the off-line dynamic vegetation model test with prescribed atmospheric states. In addition, the results from a fully interactive ESM model test with the modified  $Q_{10}$  are provided in that section. Summary and further discussion are provided in Section 4.

## **2. Data, Methods, and Experiments**

### **2.1. Data**

FLUXNET-MTE (Multi Tree Ensemble) data (Jung et al., 2009) is used to validate GPP. FLUXNET provides the global distribution of carbon and water fluxes in the vegetated land surface and its temporal variation, which were derived from upscaling eddy covariance measurements at the flux tower sites using a statistical machine-learning algorithm. The data provide the information on terrestrial carbon and water cycles globally (Jung et al. 2009). The data's spatial resolution is  $0.5^\circ \times 0.5^\circ$  (lat./lon.) and time resolution is monthly for 23 years (1983–2009).

This study also used the Moderate Resolution Imaging Spectroradiometer (MODIS) GPP and net primary production (NPP) data. Autotrophic respiration ( $R_a$ ) by plants was determined by subtracting NPP from GPP by definition. This study used the gridded data for the global domain at  $0.5^\circ \times 0.5^\circ$  horizontal resolution. These data are originally from MODIS17A3 GPP and NPP products in HDF EOS (Hierarchical Data Format – Earth Observing System) format with a native resolution of 1 km (Running et al., 2004).

When GPP is compared between in situ observation-based FLUXNET-MTE and satellite-based MODIS, the two datasets show a minor difference for the overlapping period (2000–2006). The global GPP of FLUXNET-MTE is 101.13 GtC yr<sup>-1</sup> and that of MODIS is 100.51 GtC yr<sup>-1</sup>, which is less than 1 % of the total value.

Simulations of soil respiration (Rs) by CLM4 will be verified using the gridded reanalysis dataset from Hashimoto et al. (2015), which has the data period of 1983-2005. The data were also used for the parameterization of soil respiration (described in detail in section 2.2 in Hashimoto et al., 2015). Although only directly observed soil respiration is available from soil respiration database (SRDB) version 3 (Bond-Lamberty and Thomson, 2010), it has limited sampling for boreal cold regions (i.e., tundra and northern Siberian) as well as unpopulated regions in the tropics, covering a significant portion of the global biosphere. The data from Hashimoto et al. were derived using SRDB data and the empirical soil respiration model with specified climate conditions for surface air temperature and precipitation. The model was modified and updated from the original version of Raich et al. (2002). Global land use data in a synergetic land cover product (SYNMAP, Jung et al., 2006) using a Bayesian calibration scheme were used to determine the best parameter set for deriving the climate-driven model of soil respiration. The climate-forcing data were obtained from CRU version 3.21 climate data (University of East Anglia Climatic Research Unit, 2013). These data was applied monthly at a spatial resolution of 0.5° X 0.5° (lat./lon.).

All the data were regridded onto 1.9° X 2.5° lat./lon. grids for comparison with the CLM4 simulation at this resolution.

## **2.2. Q<sub>10</sub> Parameterization**

Most dynamic vegetation models implemented in current ESMs, including CLM4, adopt a simple type of empirical equation for Rs, which is proportional to the soil decomposition flux



of carbon at the root zone. The decomposition flux is calculated by multiplying the carbon amount from **litters** by the rate scalar ( $R_{scalar}$ ), representing the effects of the physical environmental condition such as soil temperature ( $T_{scalar}$ ) and moisture ( $W_{scalar}$ ) as:

$$R_{scalar} = T_{scalar} * W_{scalar} , \quad (1)$$

where  $T_{scalar}$  is basically an exponential function of temperature from van't Hoff (1898). It is implemented in CLM4 as in the following equation:

$$T_{scalar} = Q_{10}^{\left[\frac{T_j - T_{ref}}{10}\right]}, \quad (2)$$

where  $T_j$  is the temperature at the  $j$ -th soil level, and  $T_{ref}$  is the reference temperature of 25 °C. CLM4 considers temperature for the top 5 soil levels as representing the root zone (approx. 29 cm depth).  $Q_{10}$  is specified as a constant value of 1.5 in the standard CLM4 model. The moisture scalar ( $W_{scalar}$ ) is based on Andren and Paustian (1987), which describes the **water potential for soil decomposition** as

$$W_{scalar} = \sum_{j=1}^5 \frac{\log\left(\frac{\psi_j}{\psi_{min}}\right)}{\log\left(\frac{\psi_{max}}{\psi_{min}}\right)}, \quad (3)$$

where  $\psi_j$  is the soil water potential at the level  $j$  defined from the exponential of volumetric soil moisture ( $\text{m}^3 \text{m}^{-3}$ ).  $\psi_{max}$  is the maximum potential depending on soil type, and  $\psi_{min}$  is the minimum value of -10 MPa, regardless of soil type. The range of  $W_{scalar}$  is 0 to 1 by setting to 0 when the  $\psi_j$  is below  $\psi_{min}$ , and setting to 1 when  $\psi_j$  is above  $\psi_{max}$ .

For improving the  $R_s$  parameterization in CLM4, this study considers a spatiotemporal change of  $Q_{10}$  in (2). We developed a multiple regression model for  $Q_{10}$  based on Qi et al. [2002], which assumes that the rate of  $R_s$  change depends entirely on soil temperature ( $T$ ) and soil moisture ( $M$ ). These two physical variables are well-known important factors for soil

biological processes. The fractional instantaneous change of  $R_s$  by soil temperature  $q$  is defined as

$$q(T, M) = \frac{1}{R_s} \frac{dR_s}{dT} \quad (4)$$

$Q_{10}$  is defined as the relative change of  $R_s$  at a temperature increase of 10 degrees, which can be described in the following equations:

$$Q_{10}(T, M) = \frac{R_s(T + 5, X)}{R_s(T - 5, X)} \quad , \quad (5)$$

$$Q_{10} = e^{\int_{T-5}^{T+5} q(T, X) dT} \quad , \quad (6)$$

where  $X$  is any additional independent variable to predict  $R_s$ . In this case, only soil moisture ( $M$ ) is considered. From (6),  $Q_{10}$  is a monotonic function of  $q$ , and the factor affecting  $q$  also influences  $Q_{10}$ . Therefore, the change of  $R_s$  is decomposed into the change by temperature and the change by moisture:

$$\frac{dR_s}{dT} = \frac{\partial R_s(T, M)}{\partial M} \frac{dM}{dT} + \frac{\partial R_s(T, M)}{\partial T} \quad . \quad (7)$$

Inserting (7) into (4), the equation for  $q$  is rewritten as

$$q(T, M) = \frac{1}{R_s} \left[ \frac{\partial R_s(T, M)}{\partial M} \frac{dM}{dT} + \frac{\partial R_s(T, M)}{\partial T} \right] \quad , \quad (8)$$

where  $dM/dT = -1/2.2 = -0.455$ , as suggested by Xu and Qi (2001).

Through a multiple regression analysis, the relationships between  $R_s$  and  $T$  and between  $R_s$  and  $M$  were obtained. In this study, multiple regression was conducted for each plant function type (PFT) for 16 classifications in CLM4. The  $Q_{10}$  multiple regression model developed in this study has an advantage over the treatment of constant value in the standard CLM4 model. First, the dependence of  $R_s$  on soil moisture and temperature can be dependent on PFT. In addition, this approach is able to consider the nonlinear relationship between  $R_s$  and the two major environmental variables of soil temperature and moisture, supported by

recent observational studies (Davidson et al., 1998; Raich et al., 2002).

Crucial for the parameterization of  $Q_{10}$  are the quality of the reference data and the degree of fitting for multiple regression. The observation data for  $R_S$  were obtained from Hashimoto et al. (2015) soil respiration data. The parametrization requires the dependence of soil respiration on subsurface temperature and moisture; these data are also not available from in situ observations. To obtain these variables, this study conducted the land surface reanalysis for recent 30 years (1981 – 2010), using the off-line land surface model driven by observed meteorological forcing data archived by Sheffield et al. (2006). The 3-hourly forcing data by Sheffield et al. (2006) consists of the National Centers for Environmental Prediction–National Center for Atmospheric Research reanalysis (Kalnay et al., 1996), which were corrected with independent observations. For precipitation, the daily Global Precipitation Climatology Project (GPCP, Huffman et al., 2001) data were processed into the 3-hourly data using the Tropical Rainfall Measuring Mission (TRMM: Huffman et al., 2003) 3B42RT but constraining daily mean amount from GPCP. Surface temperature was constrained by the observation from the monthly Climatic Research Unit (CRU) 2.0 product (Mitchell et al., 2004). The observed radiation was also used from the monthly NASA Langley surface radiation budget (Stackhouse et al., 2004) data. Remaining meteorological conditions such as surface wind and humidity were from the National Centers for Environmental Prediction–National Center for Atmospheric Research (NCEP-NCAR) atmospheric reanalysis. Interested readers refer to Sheffield et al. (2006) for the detail. Using this 3-hourly forcing data, this study integrated the off-line land surface model with 3-hourly time steps and at a  $0.5^\circ \times 0.5^\circ$  spatial resolution.

Figure 1 shows the r-squared values from the multiple regression for soil respiration for various PFT types. In most vegetation types, the regression by soil temperature and moisture tends to exhibit high values close to 1. The regression results are better than they are when the multi-model ensemble average of soil temperature and moisture from 13 Global Soil Wetness

Project (GSWP2) land surface model outputs (Dirmeyer et al., 2006) were applied to the multiple regression. This difference is attributed mostly to a better quality of forcing data by Sheffield et al. (2006), such as the use of daily precipitation data instead of monthly values in GSWP2 and a longer training period from 1983–2010 than was used for GSWP2 data (1986–1995). The r-square value was found to be comparable when the period of forcing data was reduced.

### 2.3. Experiments

Two sets of off-line CLM4 simulations were conducted with identical meteorological forcing for 23 years (1983–2005), where the only difference was the specification of  $Q_{10}$  in the control run (CTL) and the state-dependent  $Q_{10}$  in every time interval (EXP). The offline simulations for GPP and soil respiration are also compared with those from the fully-interactive Community Earth System Model with Biogeochemistry (CESM-BGC) model simulation that used the identical land surface model (i.e., CLM4). The dataset was obtained from Earth System Grid – Center for Enabling Technologies (ESG-CET at <http://pcmdi9.llnl.gov/>). Figure 2 shows the time average of  $Q_{10}$  values, where the geographical change is clear according to the dominant PFTs and climate conditions. Generally, the regions of lower canopy plants with cold soil temperatures exhibit relatively higher values, significantly higher than the default value of 1.5 in CTL. In contrast, the regions of lower  $Q_{10}$  values are located at low latitudes in high temperatures, such as the Amazon and the Maritime Continent. This result suggests that soil respiration is more sensitive to the change of soil temperature in boreal vegetated regions in cold climates.

The time average of the off-line simulation from the standard run (CTL) in Figure 3 is very similar to the fully interactive integration of the same model in terms of the spatial bias pattern for the terrestrial carbon fluxes, presumably inherited by the deficiencies in the parametrization

of the dynamic vegetation model. Both simulations tend to overestimate GPP over the tropics and underestimate it in high latitudes. The bias pattern of  $R_s$  is also quite similar with no significant difference. Despite the fact that in the simulated climatic condition the fully interactive run should be different from the observation used to drive the off-line CLM4, much resemblance in the terrestrial carbon–flux bias pattern suggests that the deficiency in the dynamic vegetation model is overwhelming the bias rather than that systematic error is occurring in the climate condition. Therefore, our comparison in the following sections is mostly for the off-line simulation differences between CTL and EXP.

### 3. Results

This study further compares the simulation of GPP by various ESMs in CMIP5. Figure 4 compares the zonal mean distribution of GPP averaged for 23 years (1983–2005) between FLUXNET-MTE observations and the historical emission-driven simulations by 10 CMIP5 ESMs (Table 2). Among the models, the two ESMs from CESM-BGC and NorESM share an identical dynamic vegetation model with an interactive C-N cycle (Bonan et al., 2011). The global GPP simulated by the multi-model ensemble (MME) of CMIP5 ESMs is  $119.28 \text{ GtC yr}^{-1}$ , which is a slight overestimation by  $18 \text{ GtC yr}^{-1}$  from the FLUXNET-MTE observation. Overall, MME shows realistic meridional variation with large values in the tropics and small values in high latitudes. As identified in previous studies, however, the ESMs tend to overestimate GPP significantly in the tropics (Shao et al., 2013; Anav et al., 2013). Global GPP simulated by the two ESMs with an interactive C-N cycle is lower than the remainder of the ESMs ( $-12 \text{ GtC yr}^{-1}$ ). Including typical biases of overestimation of GPP over tropical belts (20S–20N), the two models show the other GPP bias from the remainder of the ESMs, which tend to significantly underestimate GPP, even more so than other ESMs in the Northern Hemisphere high latitudes ( $> 60 \text{ N}$ ). These systematic biases are a common problem in the C-

N coupled models based on CLM4 (Bonan et al., 2011; Thornton et al., 2009). These systematic biases in the tropics and the Northern Hemisphere high latitudes are common in the C-N coupled models based on CLM4 (Bonan et al. 2009).

Figure 5a compares the  $R_s$  pattern between the observation and the offline model simulation. The simulated pattern also shows a general agreement with the observation, such as large soil respiration in warm and wet regions in low latitudes and less respiration in cold and dry regions in high latitudes. However, the simulation bias in CTL shows the uniform pattern of underestimation in almost every region except central China. This bias suggests that the parameterization of internal soil biological processes could be misrepresented in the standard CLM4 model.

The changes in  $R_s$  simulation by EXP are given in Figure 5b, in terms of global distribution as well as zonally-averaged distribution. Overall, the modification to  $Q_{10}$  tends to increase  $R_s$  in almost every region. This is an improvement from CTL, although the model now tends to overestimate  $R_s$  in some specific regions, such as the tropics and the high latitudes in the Northern Hemisphere, such as southern Siberia, Alaska and China. Overall the increase of  $R_s$  can be attributed to the increase of  $Q_{10}$  in most of the vegetated regions (Figure 2) from the standard value of 1.5. Despite the increase of  $R_s$  in EXP, the underestimation persists over the Amazon and other large biomass regions.

The sensitivity of  $Q_{10}$  parametrization depend on the surface vegetation types. For instance, boreal forest and shrub regions which has cold climate shows significant enhanced relationship between  $R_s$  and soil temperature. In contrast, temperate, tropical forest and Grass regions show relative higher positive relationship between  $R_s$  and temperature in CTL simulation comparing with EXP simulation (Table 3). Some regions in shrub and crop regions is unclear to show this relationship. Interestingly, PFTs of higher value of climatology averaged  $Q_{10}$  value (Table 1) comparing with standard value (1.5) enhanced relationship between  $R_s$  and soil temperature

such as boreal forest and boreal shrubs except for crop land. In boreal forest and shrub regions which has higher  $Q_{10}$  value comparing with global constant, the relationship between  $R_s$  and temperature in EXP are enhanced than CTL simulation. However, the tropical, temperate forests and grass regions (lower  $Q_{10}$  value than 1.5 in EXP simulation) is unclear for impacts of  $Q_{10}$  parameterization. One of possibility is that these regions are strong sensitivity of soil respiration to soil moisture. Figure S1 supported that this mechanism. In high temperature region, the sensitivity of  $R_s$  on the moisture is stronger than temperature. It reflected the unclear change of temperature sensitivity of  $R_s$  to soil temperature over tropical forest region.

Figure 7 compares the GPP bias patterns in CTL and EXP. CTL shows significant biases when sign and magnitude differ geographically. Among the biases, overestimation in the tropics and underestimation in Siberia is evident. Although the spatial structure of bias seems to be quite similar, implying intrinsic model deficiencies other than  $Q_{10}$ , EXP shows an improvement by reducing biases such as overestimation in southern Asia and China and underestimation in northern Eurasia in CTL. However, underestimation biases in the central part of North America and the Amazon are even larger in EXP. This change of spatial distribution of GPP is associated with sensitivity of  $R_s$  to soil temperature. Degradation of GPP simulation over Europe and North America is driven by the temperate plant type where the temperature sensitivity of  $R_s$  tends to decrease (Figure 6). On the other hand, the northern Eurasian and Chinese regions that have good improvement of GPP bias in EXP show an enhanced relationship between  $R_s$  and temperature. This result indicates that the change of  $R_s$  to soil temperature by  $Q_{10}$  variation affects not only the change in respiration but also the carbon production (GPP) flux. The variable  $Q_{10}$  in the parameterization of soil decomposition flux immediately affects the heterotrophic respiration from soil organic matter (SOM) as given by the model formulations in Eq. (1) and (2). Moreover, this modification changes the plant assimilation and GPP in the meantime in this carbon-nitrogen coupled model. A faster (slower)

carbon decomposition rate in the model tends to increase (decrease) nitrogen assimilation from soil to vegetation and plants, thereby increasing (decreasing) GPP. This aspect is illustrated well by comparing the turnover time of the soil carbon, which is defined as the ratio of soil carbon amount to the net primary production (NPP), between the CTL and EXP runs (Figure 8). As shown in the figure, the run with variable  $Q_{10}$  (EXP) makes shorter turnover time in northern hemisphere high latitudes and longer in the tropics compared with the control run(CTL). The shorter turnover time in high latitudes suggests the enhancement of nitrogen assimilation to vegetation in EXP, thereby enhancing net primary production by plants.

The improvement in the GPP simulation by the  $Q_{10}$  parameterization is illustrated better in Figure 9, which compares the regionally averaged GPP over major 4 regions. In the global average, EXP reduces the overestimation bias by approximately 10 % (103.81 GtC/yr) compared with CTL simulation (111.24 GtC/yr). Little plant cover over Southern Hemisphere (SH, 60S-20S) leads to a smaller contribution of global GPP. The improvement over this region is not clear in EXP. However, the overestimation bias in the tropical regions has been improved significantly. This result is caused by the suppression of the GPP amount in the Amazon region in EXP. This underestimation of GPP over the Amazon induces the improvement of the zonal mean terrestrial carbon budget in EXP. The middle latitude region (20N–60N), which is dominated by temperate forest and crop fields, also has a reduced overestimation of GPP bias compared with CTL. In addition, simulated GPP over high latitude regions ( $> 60N$ ) were improved in EXP. Those were also the common areas of bias in the interactive C-N coupled ESM run.

The modification to the soil process parameterization can affect the rest of the terrestrial carbon cycle by changing the carbon pools and nitrogen pools in the soil system needed for plant nitrogen assimilation. For detailed investigation of the impact of the  $Q_{10}$  parameterization, this study further investigates the changes in the simulated terrestrial carbon



cycle of each vegetation type. Figure 10 compares the observation and the simulations using two offline runs for GPP, autotrophic respiration by plants ( $R_a$ ), and  $R_s$  depending on the primary vegetation type. For the comparisons of GPP and  $R_a$ , satellite-based MODIS data were used as the data separated GPP and  $R_a$  over vegetation areas. In the MODIS observations, the terrestrial carbon cycle is largely contributed to by vegetation response in tropical and temperate tree regions. Vegetation types with a short canopy height and trees with deciduous leaves contribute less in terms of absolute amount of carbon fluxes, although their relative changes are not trivial. Both CTL and EXP runs capture these observed differences in the magnitude of carbon fluxes realistically. Regarding the simulation of GPP, EXP tends to reduce the biases, particularly in temperate, tropical and crop zones. EXP also improves the simulation of  $R_a$  in those regions. The improvement is most evident in  $R_s$ , where the simulated values are close to the observed values in most vegetation types.  $R_s$  by EXP has been increased in every type of vegetation from CTL, reaching values closer to the reference observation data. According to this result, although the absolute magnitude of  $R_s$  is much smaller compared with that of GPP and  $R_a$ , the modification of  $R_s$  by the  $Q_{10}$  parameterization affects the entire terrestrial carbon cycle and improves their simulations.

#### **4. Summary and Concluding Remarks**

Soil respiration is a crucial process in maintaining terrestrial carbon cycles. Although its sensitivity to the physical environmental conditions such as soil temperature and moisture depends on the type of vegetation, as supported by observational data, most contemporary ESMs do not consider this dependence. These models thereby underestimate the effects of and feedbacks from soil respiration on terrestrial carbon cycles. Using the CLM4 land surface model with the interactive C-N cycle, this study developed a new parameterization method to consider the spatiotemporal variation of  $Q_{10}$  that represents the sensitivity of soil respiration to

the temperature change for each different vegetation type. This sensitivity has been treated as constant with a uniform value regardless of plant type in the original CLM4 model.

The new parameterization changes the simulation of soil respiration and the rest of terrestrial carbon fluxes significantly by enhancing the feedback to the plant production process. The new parameterization calculates  $Q_{10}$  at every time interval for each location, and this state-dependent prescription induces the overall increase of soil respiration in most locations and most vegetation types, improving spatially uniform negative bias in the original CLM4 simulation with constant  $Q_{10}$  value. The simulated sensitivity of soil respiration to soil temperature and moisture by the new method showed more realistic features, particularly in the temperate and cold regions. This changed soil carbon fluxes at the subsurface and affected the simulation of GPP, where the simulation of spatial distribution of GPP has been improved particularly over high latitudes with short canopy heights and over the tropics and warm regions, including southern Asia and China. The improved GPP simulation over cold regions was mostly attributed to the increase in carbon decomposition in those regions. Due to the advancement of both respiration and primary production, carbon balance between subsurface and surface ecosystems with soil organic matter and plants were also improved by the new  $Q_{10}$  parameterization. The observed ratio of soil respiration to GPP was represented better in the new simulation, which clearly shows the dependence on the vegetation type.

The major findings from this study suggest that the modification of subsurface terrestrial carbon cycle processes is important for improving the simulation of terrestrial carbon fluxes. The parameterization of the photosynthetic process is still a major term crucially related to primary production (Bonan et al. 2010; Bonan et al., 2011). Previous studies have suggested that the improvement of canopy processes in the photosynthetic parameter in CLM4 was able to improve the simulation by reducing the overestimation of GPP in the tropics. Despite the improvement in the photosynthetic process in their models, respiration processes by plants and

soil are still largely uncertain due to a lack of reliable observational data and comprehensive studies (Bonan et al. 2010; Bonan et al., 2011). For this reason, this study approached the modification of the soil decomposition process, aiming to improve the terrestrial carbon cycle.

In fact, the parameterization of photosynthesis in the state-of-the-art ESMs is implemented in a similar fashion with small differences, based on the formulations from Farquhar et al. (1980).

Still, large uncertainties lie in the formulation of the respiration process and its parameters. This study suggested that the improved soil decomposition process induces a change in carbon-climate feedback intensity by changing soil respiration. In addition, the realistic description of  $Q_{10}$  variation in a numerical model will reduce the uncertainty of the magnitude of carbon-climate feedback due to accurate atmospheric CO<sub>2</sub> simulation in ESMs.

## Acknowledgement

This study is supported Basic Science Research Program through the National Research Foundation of Korea (NRF), funded by the Ministry of Education, Science and Technology (2012M1A2A2671851) and the Supercomputing Center/Korea Institute of Science and Technology Information with supercomputing resources including technical support (KSC-2015-C3-035).

## References

- Anav, A., Friedlingstein, P., Kidston, M., Bopp, L., Ciais, P., Cox, P., Jones, C., Jung, M., Myneni, R., and Zhu, Z.: Evaluating the land and ocean components of the global carbon cycle in the CMIP5 Earth System Models, *J. Clim.*, 26, 6801–6843, doi:10.1175/JCLI-D-12-00417.1, 2013.
- Andren, O., Paustian, K.: Barley Straw Decomposition in the Field: A Comparison of Models, *Biology*, 68, 1190-1200, doi:10.2307/1939203, 1987.
- Arora, V. K., Boer, G. J., Friedlingstein, P., Eby, M., Jones, C. D., Christian, J. R., Bonan, G., Bopp, L., Brovkin, V., Cadule, P., Hajima, T., Ilyina, T., Lindsay, K., Tjiputra, J. F., Wu, T.: Carbon–concentration and carbon–climate feedbacks in CMIP5 earth system models, *J. Clim.*, 26, 5289-5314, doi:10.1175/JCLI-D-12-00494.1, 2013.
- Beer, C., Reichstein, M., Tomelleri, E., Ciais, P., Jung, M., Carvalhais, N., Rodenbeck, C., Arain, M. A., Baldocchi, D., Bonan, G. B., Bondeau, A., Cescatti, A., Lasslop, G., Lindroth, A., Lomas, M., Luyssaert, S., Margolis, H., Oleson, K. W., Rouspard, O., Veenendaal, E., Viovy, N., Williams, C., Woodward, F. I., and Papale, D.: Terrestrial Gross Carbon Dioxide Uptake: Global Distribution and Covariation with Climate, *Science*, 329, 834-838, 2010.
- Belay-Tedla, A., Zhou, X. H., Su, B., Wan, S. Q., and Luo, Y. Q.: Labile, recalcitrant, and microbial carbon and nitrogen pools of a tallgrass prairie soil in the US Great Plains subjected to experimental warming and clipping, *Soil Biol. Biochem.*, 41, 110–116, 2009.
- Bonan, G. B.: Forests and Climate Change: Forcings, Feedbacks, and the Climate Benefits of Forests, *Science*, 320, 1444-1449, 2008.
- Bonan, G. B., Lawrence, P. J., Oleson, K. W., Levis, S., Jung, M., Reichstein, M., Lawrence, D. M., and Swenson, S. C.: Improving canopy processes in the Community Land Model version 4 (CLM4) using global flux fields empirically inferred from FLUXNET data, *J. Geophys. Res.*, 116, G02014, doi:10.1029/2010JG001593, 2011.

Bonan, G. B., and Levis S.: Quantifying carbon-nitrogen feedbacks in the Community Land Model (CLM4), *Geophys. Res. Lett.*, 37, L07401, doi:10.1029/2010GL042430, 2010.

Bond-Lamberty, B., and Thomson, A.: Temperature-associated increases in the global soil respiration record., *Nature*, 464, 579-582, doi:10.1038/nature08930, 2010.

Booth, B. B. B., Jones, C. D., Collins, M., Totterdell, I. J., Cox, P. M., Sitch, S., Huntingford, C., Betts, R. A., Harris, G. R., and Lloyd, J.: High sensitivity of future global warming to land carbon cycle processes, *Environ. Res. Lett.*, 7, 024002, doi:10.1088/1748-9326/7/2/024002, 2012.

Cox, P. M., Betts, R. A., Jones, C. D., Spall, S. A., Totterdell, I. J., :Acceleration of global warming due to carbon-cycle feedbacks in a coupled climate model, *Nature*, 408, 184-187, 2000.

Davidson, E. A., Belk, E., and Boone, R. D.: Soil water content and temperature as independent or confounded factors controlling soil respiration in a temperate mixed hardwood forest, *Global change biol.*, 4, 217-227, doi: 10.1046/j.1365-2486.1998.00128.x, 1998.

Davidson, E. A. and Janssens, I. A.: Temperature sensitivity of soil carbon decomposition and feedbacks to climate change., *Nature*, 440, 165–173, doi:10.1038/nature04514, 2006.

Davidson, E. A., Janssens, I. A. and Luo, Y.: On the variability of respiration in terrestrial ecosystems: moving beyond Q10, *Glob. Chang. Biol.*, 12(2), 154–164, doi:10.1111/j.1365-2486.2005.01065.x, 2006.

Dufresne J. L., Friedlingstein, P., Berthelot, M., Bopp, L., Ciais, P., Fairhead, L., Le Treut, H., Monfray, P.: On the magnitude of positive feedback between future climate change and the carbon cycle, *Geophys. Res. Lett.*, 29, 1405, 43 , 2002.

Farquhar G. D., Caemmerer, S., Berry, J. A.:A biochemical model of photosynthetic CO<sub>2</sub> assimilation in leaves of C<sub>3</sub> species, *Planta*, 149, 78–90, 1980.

513      Foley, J. A., Levis, S., Prentice, I. C.: Coupling dynamic models of climate and vegetation,  
514      Global Change Biol., 4, 561–79, 1998.

515      Friedlingstein, P., Cox, P., Betts, R., Bopp, L., von Bloh, W., Brovkin, V., Cadule, P., Doney,  
516      S., Eby, M., Fung, I., Bala, G., John, J., Jones, C., Joos, F., Kato, T., Kawamiya, M., Knorr, W.,  
517      Lindsay, K., Matthews, H. D., Raddatz, T., Rayner, P., Reick, C., Roeckner, E., Schnitzler, K.  
518      G., Schnur, R., Strassmann, K., Weaver, A. J., Yoshikawa, C., and Zeng, N.: Climate–carbon  
519      cycle feedback analysis: Results from the C4MIP model intercomparison, J. Clim., 19, 3337–  
520      3353, doi:10.1175/JCLI3800.1, 2006.

521      Friedlingstein P., Dufresne, J. L., Cox, P. M., Rayner, P.: How positive is the feedback  
522      between climate change and the carbon cycle?, Tellus-B, 55, 692–700,2003

523      Friedlingstein, P., Meinshausen, M., Arora, V. K., Jones, C. D., Anav, A., Liddicoat, S. K.,  
524      and Knutti, R.: Uncertainties in CMIP5 climate projections due to carbon cycle feedbacks, J.  
525      Clim., 27, 511-525, doi:10.1175/JCLI-D-12-00579.1, 2014.

526      Gregory, J. M., Jones, C. D., Cadule P., and Friedlingstein P.: Quantifying Carbon Cycle  
527      Feedbacks, J. Clim., 22, 5232-5249, 2009.

528      Hashimoto, S., Carvalhais, N., Ito, A., Migliavacca, M., Nishina, K., and Reichstein, M.:  
529      Global spatiotemporal distribution of soil respiration modeled using a global database,  
530      Biogeosciences, 12, 4121-4132, doi:10.5194/bg-12-4121-2015, 2015.

531      Hoffman, F. M., Randerson, J. T., Arora, V. K., Bao, Q., Cadule, P., Ji, D., Jones, C. D.,  
532      Kawamiya, M., Khatiwala, S., Lindsay, K., Obata, A., Shevliakova, E., Six, K. D., Tjiputra, J.  
533      F., Volodin, E. M., and Wu, T.: Causes and implications of persistent atmospheric carbon  
534      dioxide biases in Earth System Models, J. Geophys. Res. Biogeosci., 119, 141-162, doi:  
535      10.1002/2013JG002381, 2013.

536      Jung, M., Henkel, K., Herold, M., and Churkina, G.: Exploiting synergies of global land  
537      cover products for carbon cycle modeling, Remote. Sens. Environ., 101, 534–553, 2006.

Jung., M., Reichstein, M., and Bondeau, A.: Towards global empirical upscaling of FLUXNET eddy covariance observations: validation of a model tree ensemble approach using a biosphere model, *Biogeosciences*, 6, 2001–2013, doi:10.5194/bg-6-2001-2009, 2009.

Karhu, K., Auffret, M. D., Dungait, J. A. J., Hopkins, D. W., Prosser, J. I., Singh, B. K., Subke, J.-A., Wookey, P. A., Ågren, G. I., Sebastià, M.-T., Gouriveau, F., Bergkvist, G., Meir, P., Nottingham, A. T., Salinas, N. and Hartley, I. P.: Temperature sensitivity of soil respiration rates enhanced by microbial community response, *Nature*, 513(7516), 81–84, doi:10.1038/nature13604, 2014. \

Kirschbaum, M. U. F.: The temperature dependence of soil organic matter decomposition, and the effect of global warming on soil organic C storage, *Soil Biol. Biochem.*, 27, 753–760, 1995.

Kutsch, W. L., Bahn, M., and Heinemeyer, A.: Soil carbon dynamics: An integrated methodology, Cambridge: Cambridge University Press., 2009

Le Quéré, C., Raupach, M. R., Canadell, J. G., Marland, G., Bopp, ' L., Ciais, P., Conway, T. J., Doney, S. C., Feely, R. A., Foster, P., Friedlingstein, P., Gurney, K., Houghton, R. A., House, J. I., Huntingford, C., Levy, P. E., Lomas, M. R., Majkut, J., Metzl, N., Ometto, J. P., Peters, G. P., Prentice, I. C., Randerson, J. T., Running, S. W., Sarmiento, J. L., Schuster, U., Sitch, S., Takahashi, T., Viovy, N., van der Werf, G. R., and Woodward, F. I.: Trends in the sources and sinks of carbon dioxide, *Nat. Geosci.*, 2, 831–836, doi:10.1038/ngeo689, 2009.

Liski, J., Ilvesniemi, H., Makel, A., Westman, K. J.: CO<sub>2</sub> emissions from soil in response to climatic warming are overestimated – the decomposition of old soil organic matter is tolerant of temperature, *Ambio*, 28, 171–174, 1999.

Lloyd, J. and Taylor, J. A.: On the Temperature Dependence of Soil Respiration, *Funct. Ecol.*, 8, 315–323, 1994.

Luo, Y., Wan, S., Hui, D., and Wallace, L. L.: Acclimatization of soil respiration to warming

in a tall grass prairie, *Nature*, 413, 622-625, doi:10.1038/35098065, 2001.

Luyssaert, S., Inglima, I., and Jung M.: The CO<sub>2</sub>-balance of boreal, temperate and tropical forest derived from a global database, *Global Change Biol*, 13, 2509-2537, 2007.

Mahecha, M. D., Reichstein, M., Carvalhais, N., Lasslop, G., Lange, H., Seneviratne, S. I., Vargas, R., Ammann, C., Arain, M. A., Cescatti, A., Janssens, I. A., Migliavacca, M., Montagnani, L. and Richardson, A. D.: Global convergence in the temperature sensitivity of respiration at ecosystem level, *Science*, 329, 838–840, doi:10.1126/science.1189587, 2010.

Malhi, Y., Baldocchi, D. D., and Jarvis, P. G.: The carbon balance of tropical, temperate and boreal forests, *Plant, cell and environ.*, 22, 715-740, 1999.

Mao, J., Thornton, P. E., Shi, X., Zhao, M., and Post, W. M.: Remote Sensing Evaluation of CLM4 GPP for the Period 2000–09, *J. Clim.*, 25, 5327-5342, doi: <http://dx.doi.org/10.1175/JCLI-D-11-00401.1>, 2012.

Oleson, K., Lawrence, D. M., Bonan, G. B., Drewniak, B., Huang, M., Koven, C. D., Levis, S., Li, F., Riley, W. J., Subin, Z. M., Swenson, S. C., Thornton, P. E., Bozbiyik, A., Fisher, R., Heald, C. L., Kluzek, E., Lamarque, J.-F., Lawrence, P. J., Leung, L. R., Lipscomb, W., Muszala, S., Ricciuto, D. M., Sacks, W., Sun, Y., Tang, J., and Yang, Z.-L.: Technical Description of version 4.5 of the Community Land Model (CLM), NCAR Technical Note NCAR/TN-503+STR, Boulder, Colorado, 420 pp., 2013.

Qi, Y., Xu, M., and Wu, J.: Temperature sensitivity of soil respiration and its effects on ecosystem carbon budget: nonlinearity begets surprises, *Ecolog. Model.*, 153, 131–142, 2002.

Raich, J. W., Potter, C. S., and Bhagawati, D.: Interannual variability in global soil respiration, 1980–1994, *Glob. Change Biol.*, 8, 800–812, 2002.

Reichstein, M., Tenhunen, J. D., Rouspard, O., Ourcival, J. -M., Rambal, S., Dore, S., and Valentini, R.: Ecosystem respiration in two Mediterranean evergreen Holm Oak forests: drought effects and decomposition dynamics, *Funct. Ecolo.*, 16, 27–39, doi: 10.1046/j.0269-



588 8463.2001.00597.x, 2002.

589 Running, S. W., Nemani, R. R., Heinsch, F. A., Zhao, M., Reeves, M., and Hashimoto, H.:  
590 A Continuous Satellite-Derived Measure of Global Terrestrial Primary Production, *BioScience*,  
591 54(6), 547-560, 2004.

592 Shao P., Zeng, X., Sakaguchi, K., Monson, R. K., and Zeng, X.: Terrestrial carbon cycle:  
593 climate relations in eight CMIP5 earth system models, *J. Clim.*, 26, 8744-8764,  
594 doi:10.1175/JCLI-D-12-00831.1, 2013.

595 Seller, P. J., Mintz, Y., Sud Y. C., and Dalcher, A.: A simple biosphere model (SiB) for use  
596 within general circulation models, *J. Atmos. Sci.*, 43, 505–531, doi:10.1175/1520-  
597 0469(1986)043<0505:ASBMFU>2.0.CO;2., 1986.

598 Sheffield, J., Goteti, G., and Wood, E. F.: Development of a 50-Year High-Resolution Global  
599 Dataset of Meteorological Forcings for Land Surface Modeling, *J. Clim.*, 19, 3088-3111  
600 doi: <http://dx.doi.org/10.1175/JCLI3790.1>, 2006.

601 Sitch, S., Smith, B., Prentice, I. C., Areneth, A., Bondeau, A., Cramer, W., Kaplan, J. O.,  
602 Levis, S., Lucht, W., Sykes, M. T., Thonicke, K., and Venevsky, S.: Evaluation of ecosystem  
603 dynamics, plant geography and terrestrial carbon cycling in the LPJ dynamic global vegetation  
604 model, *Global Change Biol.*, 9, 161-185, 2003.

605 Suseela, V., Conant, R. T., Wallenstein, M. D., and Dukes, J. S.: Effects of soil moisture on  
606 the temperature sensitivity of heterotrophic respiration vary seasonally in an old-field climate  
607 change experiment, *Global Change Biol.*, 18, 336–348, 2012.

608 Tang, J., and Baldocchi, D. D.: Spatial–temporal variation in soil respiration in an oak–grass  
609 savanna ecosystem in California and its partitioning into autotrophic and heterotrophic  
610 components, *Biogeochem.*, 73, 183–207, 2005.

611 Taylor, B. R., Parkinson, D., and Parsons, W. F. J.: Nitrogen and Lignin Content as Predictors  
612 of Litter Decay Rates: A Microcosm Test, *Ecology*, 70, 97-104.

613 Doi:<http://dx.doi.org/10.2307/1938416>, 1989.

614 Thornton, P. E., Doney, S. C., Lindsay, K., Moore, J. K., Mahowald, N., Randerson, J. T.,  
615 Fung, I., Lamarque, J.-F., Feddesma, J. J., and Lee, Y. -H.: Carbon-nitrogen interactions regulate  
616 climate-carbon cycle feedbacks: results from an atmosphere-ocean general circulation model,  
617 *Biogeosciences*, 6, 2099–2120, 2009.

618 Trumbore, S.: Carbon respired by terrestrial ecosystems – recent progress and challenges,  
619 *Global Change Biol.*, 12, 141-153, DOI: 10.1111/j.1365-2486.2006.01067.x, 2006.

620 University of East Anglia Climatic Research Unit (CRU) [Jones Phil and Harris Ian]: CRU  
621 TS3.21: Climatic Research Unit (CRU) Time-Series (TS) Version 3.21 of High Resolution  
622 Gridded Data of Month-by-month Variation in Climate (Januray 1901–December 2012),  
623 doi:10.5285/D0E1585D-3417-485F- 87AE-4FCECF10A992, 2013.

624 van't Hoff, J. H.: *Lectures on Theoretical and Physical Chemistry. Part I. Chemical Dynamics*,  
625 Edward Arnold, London, 224-229, 1898.

626 Wan, S., and Luo Y.: Substrate regulation of soil respiration in a tallgrass prairie: Results of  
627 a clipping and shading experiment, *Global Biogeochem. Cy.*, 17, 1054,  
628 doi:10.1029/2002GB001971., 2003.

629 Wang, Y. P., Law, R. M., and Pak, B.: A global model of carbon, nitrogen and phosphorus  
630 cycles for the terrestrial biosphere, *Biogeosciences*, 7, 2261–2282, doi:10.5194/bg-7-2261-  
631 2010, 2010.

632 Xu, M., and Qi, Y.: Spatial and seasonal variations of  $Q_{10}$  determined by soil respiration  
633 measures at a Sierra Nevadan forest, *Global Biogeochem. Cy.*, 15, 687 – 696, 2001.

634 Zhao, M. S., Heinsch, F. A., Nemani, R. R., and Running, S.W.: Improvements of the  
635 MODIS terrestrial gross and net primary production global data set, *Remote Sens. Environ.*,  
636 95, 164–176, doi:10.1016/j.rse.2004.12.011, 2005.

637 Zhou, T., Shi, P., Hui, D., and Luo, Y.: Global pattern of temperature sensitivity of soil

638 heterotrophic respiration ( $Q_{10}$ ) and its implications for carbon-climate feedback, J. Geophys.  
639 Res., 114, doi:10.1029/2008JG000850, 2009.

640

641

642

**Table 1.** Climatological averaged  $Q_{10}$  values by PFTs in CLM4

	Temperate	Boreal	Tropical	Shrub	B. Shrub	Grass	Crop
Averaged $Q_{10}$ value	1.446	1.762	1.374	1.266	1.918	1.842	2.041

**Table 2. List of ESMs used in this study and their features**

Nu mb er	Models	Modeling center	Horizontal resolution	ESM Reference	Land model	Photosynthesis	Autotropic Respiration	Nitrogen Cycle	Dynamic Vegetation
1	BCC- CSM 1	Beijing Climate Center, China	$2.812^{\circ} \times$ $2.812^{\circ}$	Wu et al. (2013)	BCC- AVIM1	Farquhar et al., (1980)	Foley et al. (1996)	No	No
2	BCC- CSM 1M	Beijing Climate Center, China	$1.125^{\circ} \times$ $1.125^{\circ}$	Wu et al. (2013)	BCC- AVIM1	Farquhar et al., (1980) Collatz et al. (1992)	Foley et al. (1996)	No	No
3	CanES M2	Canadian Centre for Climate Modeling and Analysis, Canada	$2.812^{\circ} \times$ $2.812^{\circ}$	Arora et al. (2011)	CTEM	Farquhar et al., (1980) Collatz et al. (1992)	Ryan (1991)	No	No
4	CESM1 - BGC	Community Earth System Model Contributors, NSF-DOE-NCAR, USA	$1.25^{\circ}$ $\times 0.9^{\circ}$	Long et al. (2013)	CLM4	Farquhar et al., (1980) Collatz et al. (1992)	Foley et al. (1996)	Yes	No
5	GFDL- ESM2M	NOAA Geophysical Fluid Dynamics Laboratory, USA	$2.5^{\circ} \times 2^{\circ}$	Dunne et al. (2013)	LM3	Farquhar et al., (1980) Collatz et al. (1992)	Foley et al. (1996)	No	Yes
6	GFDL- ESM2G	NOAA Geophysical Fluid Dynamics Laboratory, USA	$2.5^{\circ} \times 2^{\circ}$	Dunne et al. (2013)	LM3	Farquhar et al., (1980) Collatz et al. (1992)	Ryan (1991)	No	Yes
7	MIROC -ESM	Japan Agency for Marine-Earth Science	$2.812^{\circ} \times$ $2.812^{\circ}$	Watanabe et al. (2011)	MATSIR O+ SEIB-	Farquhar et al., (1980)	Ryan (1991)	No	No

		and Technology, Atmosphere and Ocean Research Institute, and National Institute for Environmental Studies, Japan			DGVM				
8	MPI- ESM LR	Max Planck Institute for Meteorology, Germany	$2.812^{\circ} \times$ $2.812^{\circ}$	Ilyina et al. (2013)	JSBACH	Farquhar et al., (1980)	Obata (2007)	No	Yes
9	MRI- ESM1	Meteorological Research Institute, Japan	$1.125^{\circ}$ $\times 1.125^{\circ}$	Yukimoto et al. (2011)	HAL	Farquhar et al., (1980) Collatz et al. (1992)	Ryan (1997)	No	No
10	NorES M1- ME	Norwegian Climate Centre, Norway	$2.5^{\circ}$ $\times 1.875^{\circ}$	Tjiputra et al. (2013)	CLM4	Farquhar et al., (1980) Collatz et al. (1992)	Foley et al. (1996)	Yes	No

654

655

656

657

**Table 3.** R-squared values between log Rs and soil temperature by PFTs in CTL and EXP

	Temperate	Boreal	Tropical	Shrub	B. Shrub	Grass	Crop
CTL	0.40	0.06	0.34	0.06	0.04	0.38	0.27
EXP	0.36	0.21	0.31	0.05	0.19	0.28	0.31

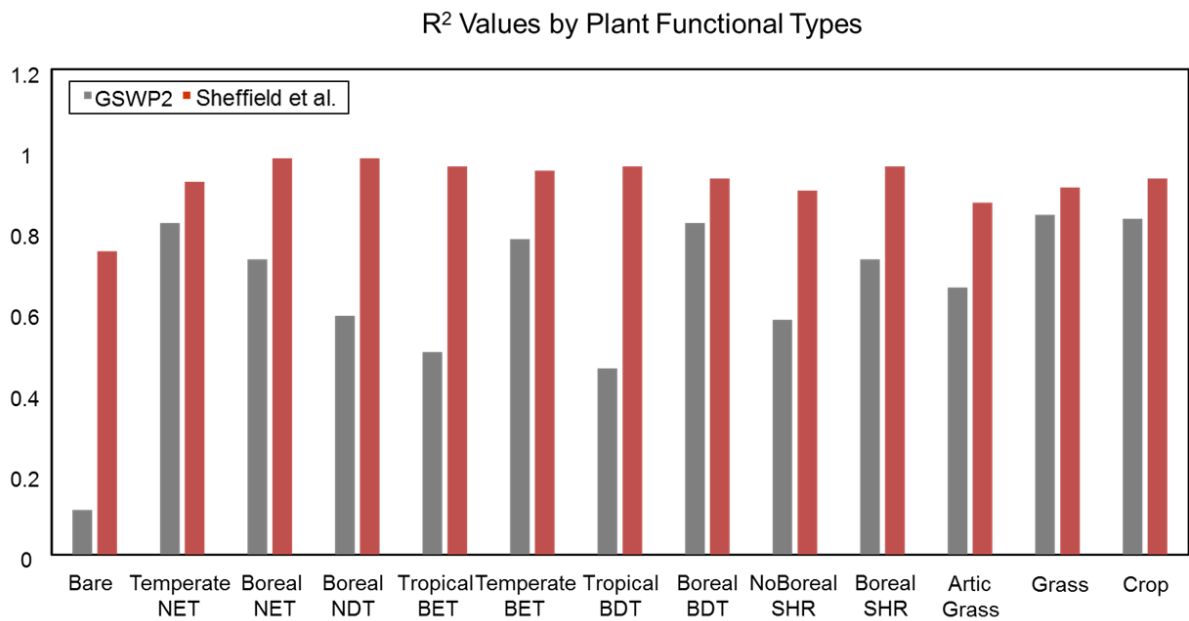
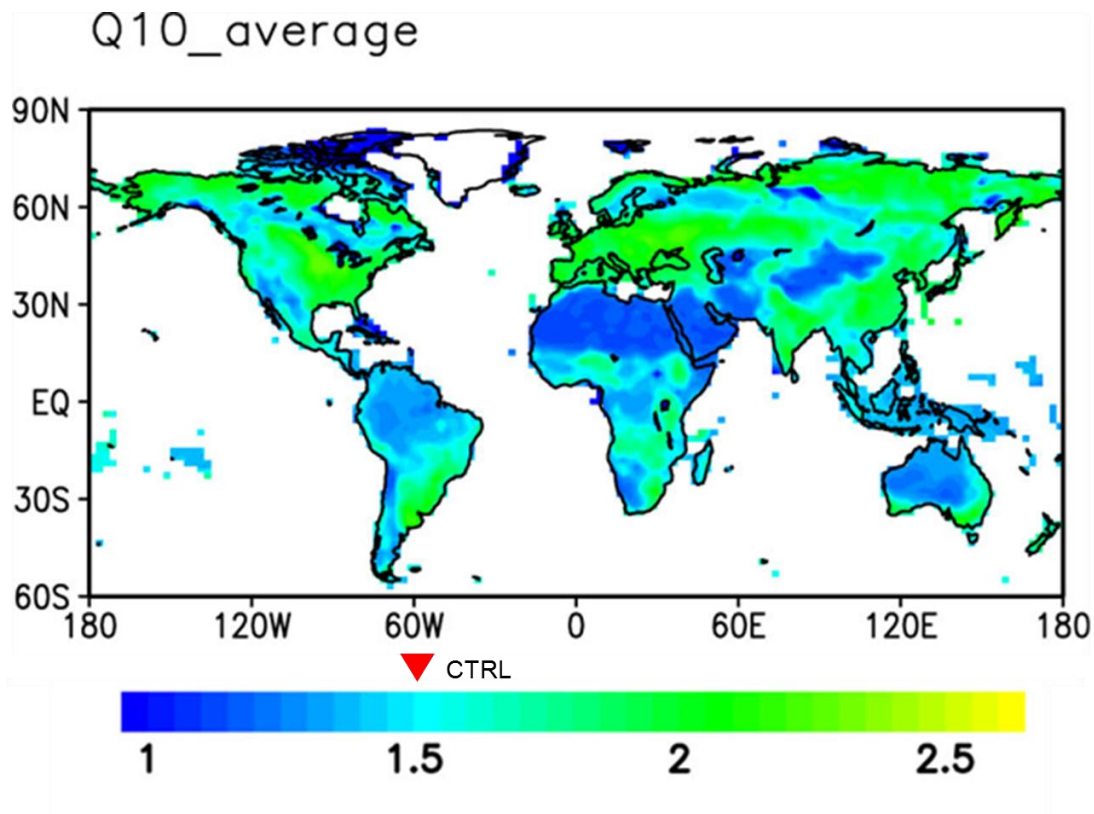


**Figure 1.** R-squared value in multiple regression by PFTs in CLM4 between soil respiration data and soil temperature and moisture from GSWP2 multiple ensemble model data (grey bars) and off-line model output forced by Sheffield data for 28 years (red bars).



677



678

679 **Figure 2.** Climatological averaged  $Q_{10}$  spatial distribution in EXP experiment. Red filled  
680 triangle indicates standard value of  $Q_{10}$  in CTL experiment.

681

682

683

684

685

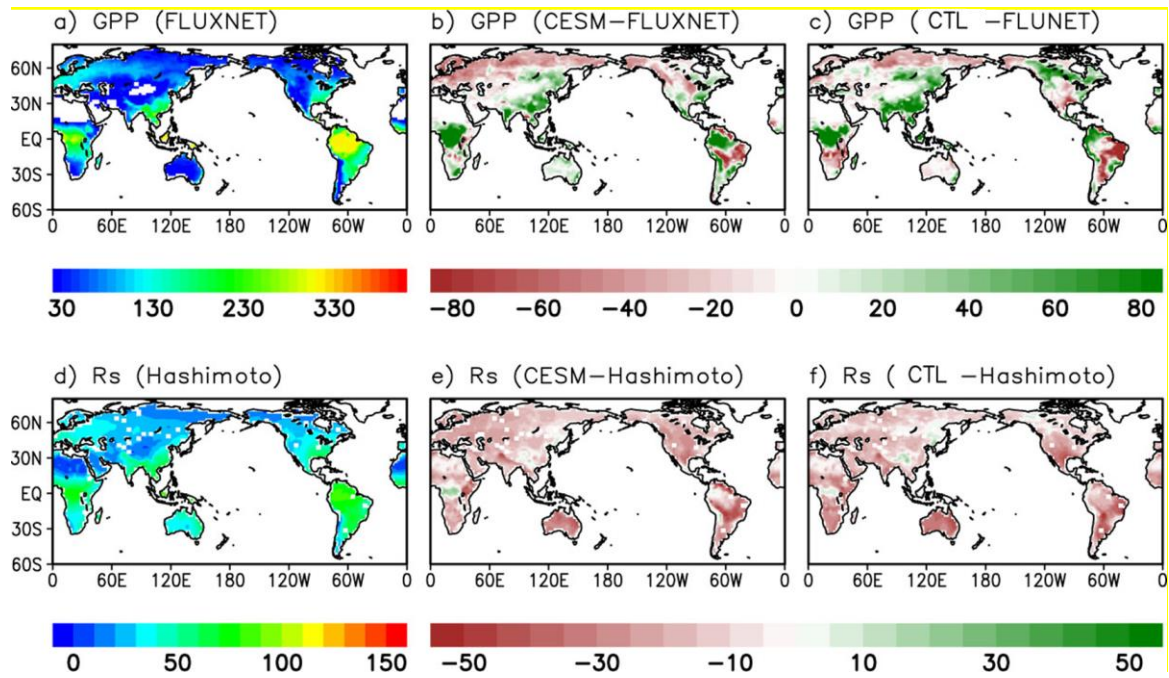


**Figure 3.** Spatial distribution of GPP(upper) and Rs (bottom) in the observation and bias patterns of online full interactive simulation (CESM) and off-line (CTR) experiment for 23 years (1983-2005). The unit is  $\text{gC m}^2 \text{mon}^{-1}$ .

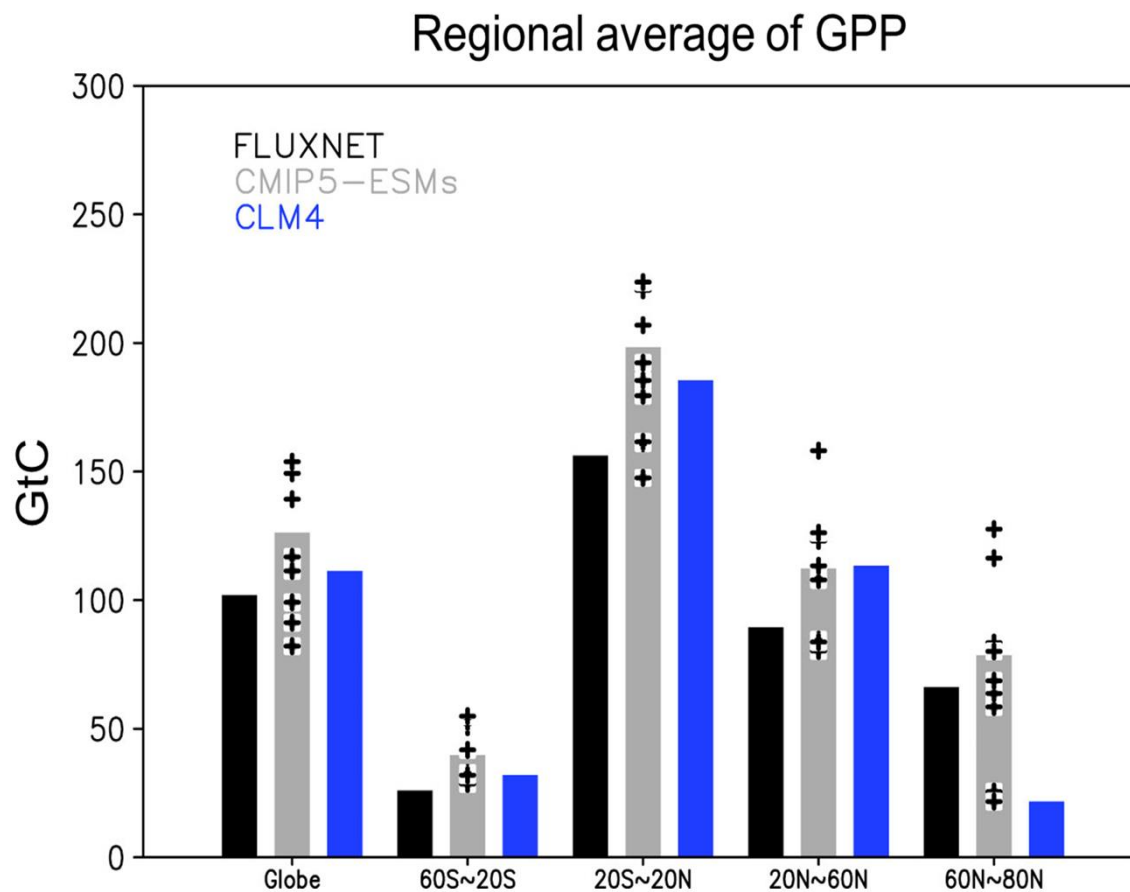
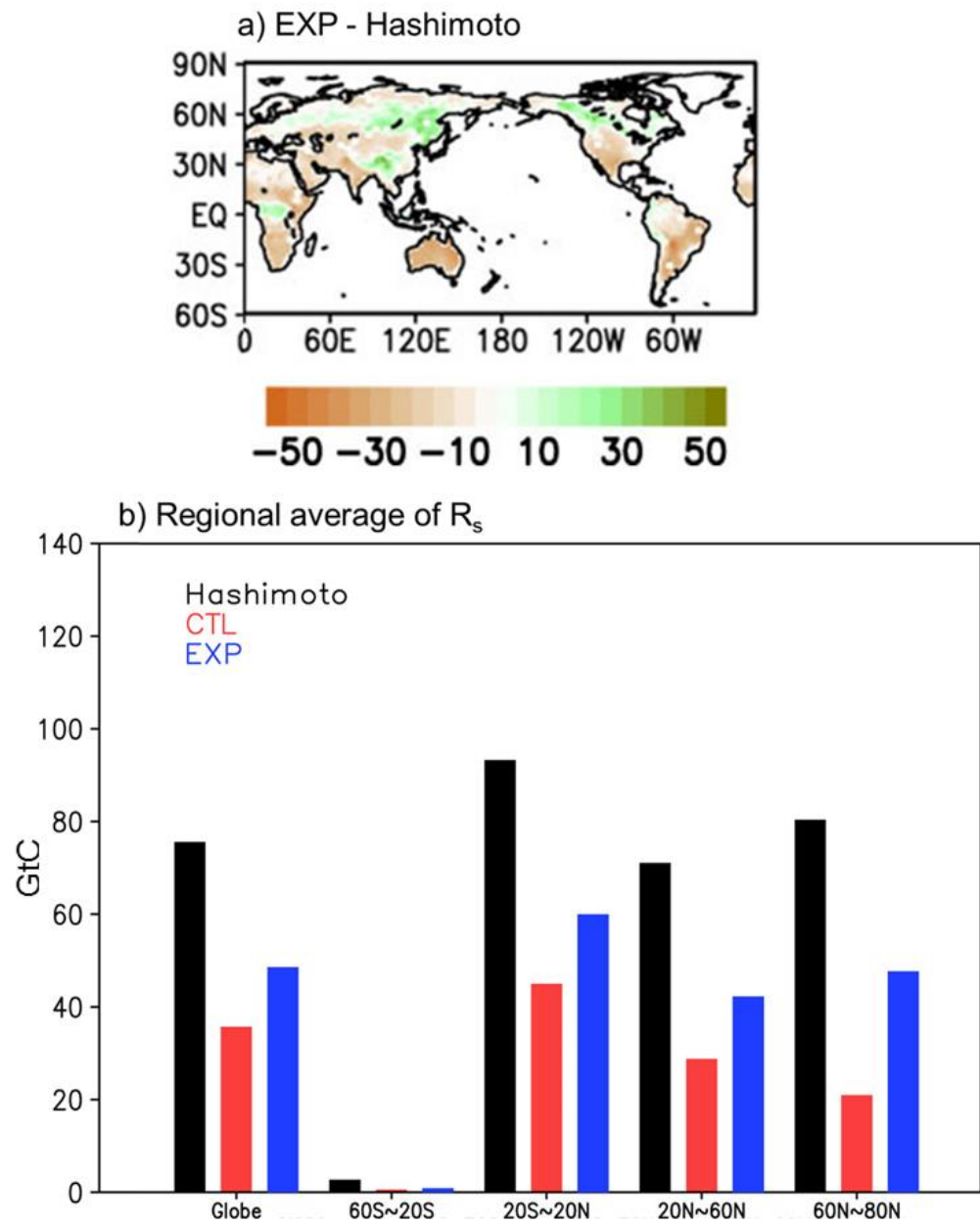


**Figure 4.** Regional averaged GPP in CMIP5 historical runs for 23 years (1983~2005). Black bars indicate the FLUXNET. Grey bars are multi-model ensemble (MME) mean of 10 CMIP5-ESMs and symbol dots are individual models. Blue bars show average of GPP simulated by ESMs which are coupled with CLM4 (CESM-BGC and NorESM).

701



702

703 **Figure 5.** (a) shows the spatial distribution of bias pattern of  $R_s$  in EXP simulation. The

704 unit is  $\text{gC m}^2 \text{ mon}^{-1}$ . (b) indicates the comparison of the regional average of  $R_s$  between

705 Hashimoto data (black bars), CTL simulation (red bars) and EXP experiment (blue bars).

706

707

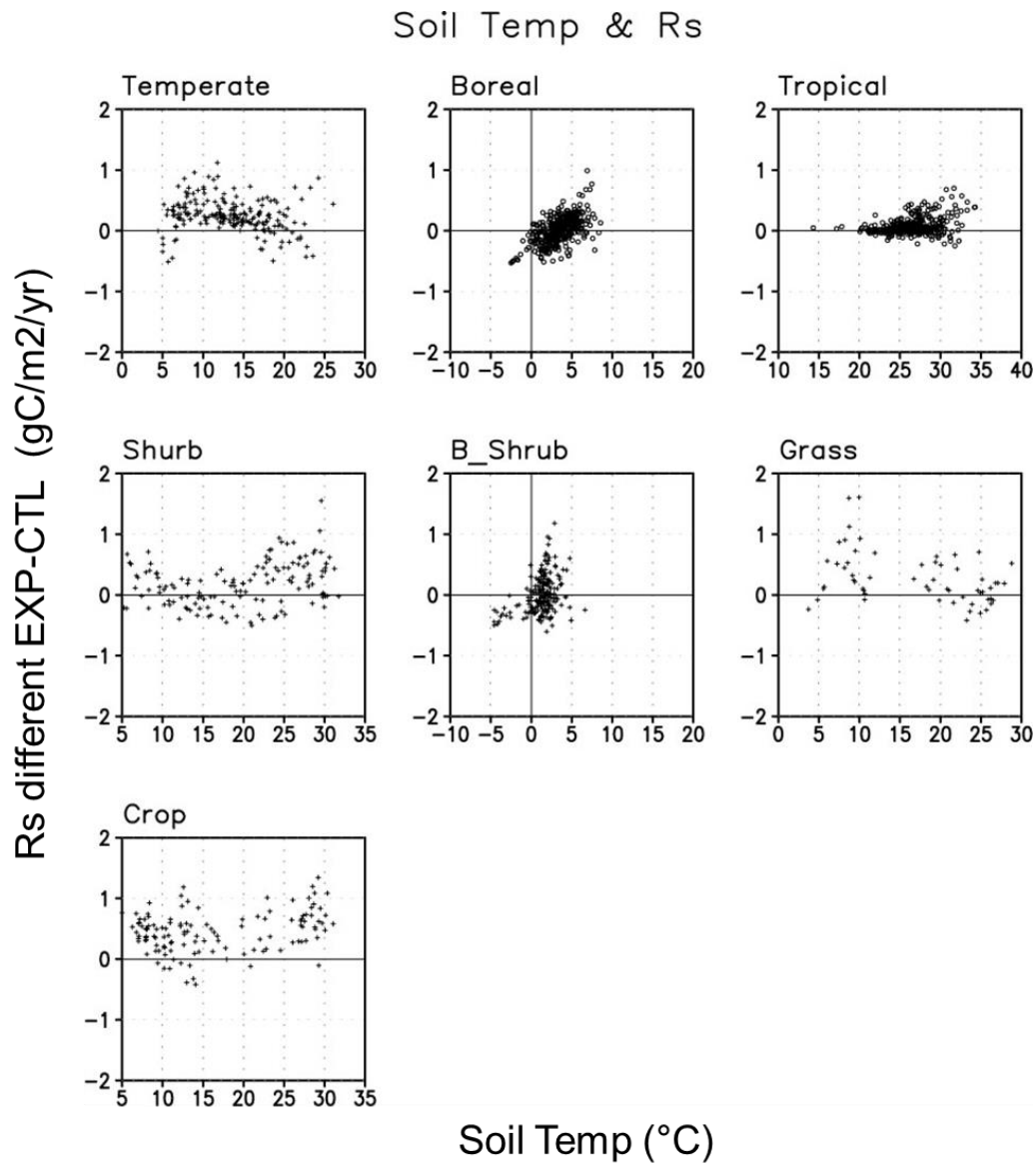


**Figure 6.** Scatter plots of change of Rs (y-axis) between EXP and CTL simulation as a function of soil temperature (x-axis). Each panel shows the plots for different PFTs that include temperate (temperate NET and BET), boreal (boreal NET, NDT, BDT), tropical (toprical BET, BDT), Shrub, B\_shrub (Boreal shrub), Grass(Grass) and Crop(Crop).

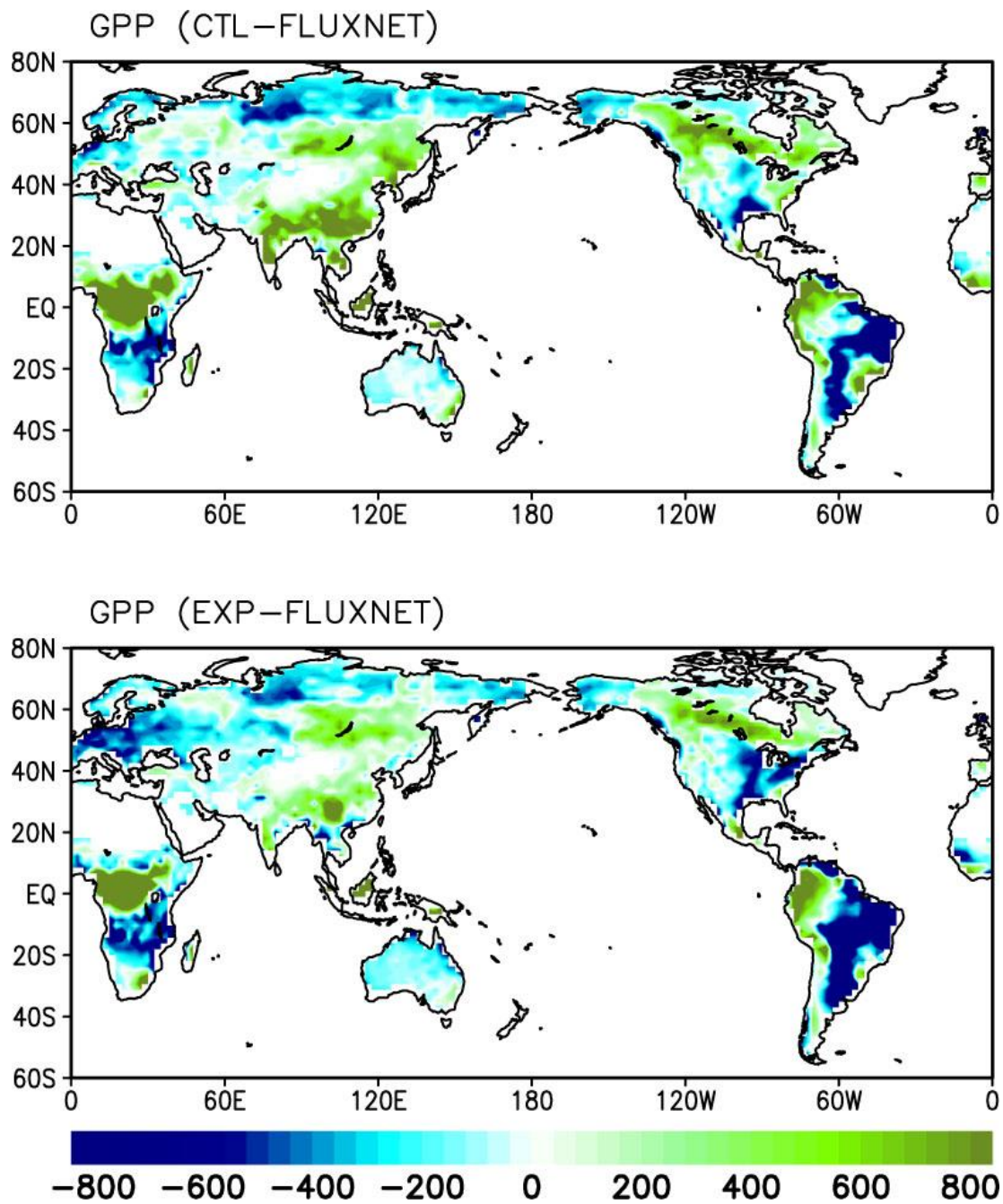


**Figure 7.** Bias of GPP spatial distribution in CTL and EXP comparing with FLUXNET during 23 years (1983-2005). Unit is gC/m2/yr.

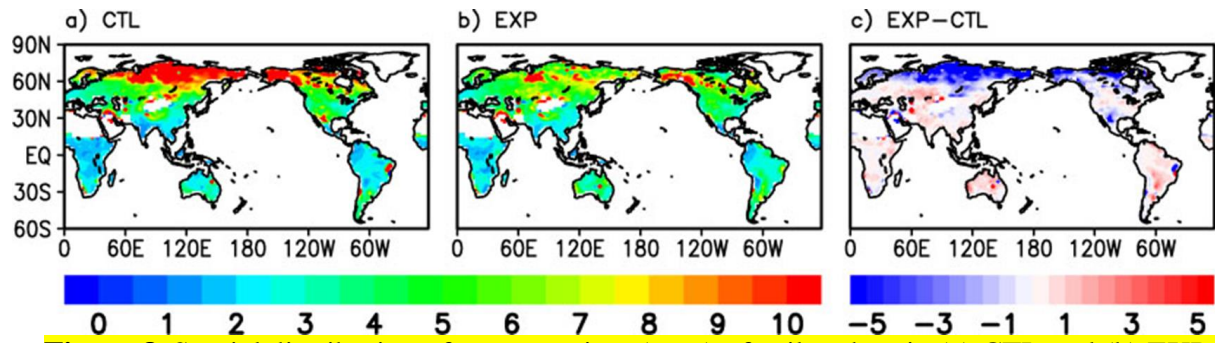


**Figure 8.** Spatial distribution of turnover time (year) of soil carbon in (a) CTL and (b) EXP.

(c) indicates the difference between EXP and CTL simulation. The turnover time is defined as the ratio of the soil carbon amount to the net primary production (NPP).

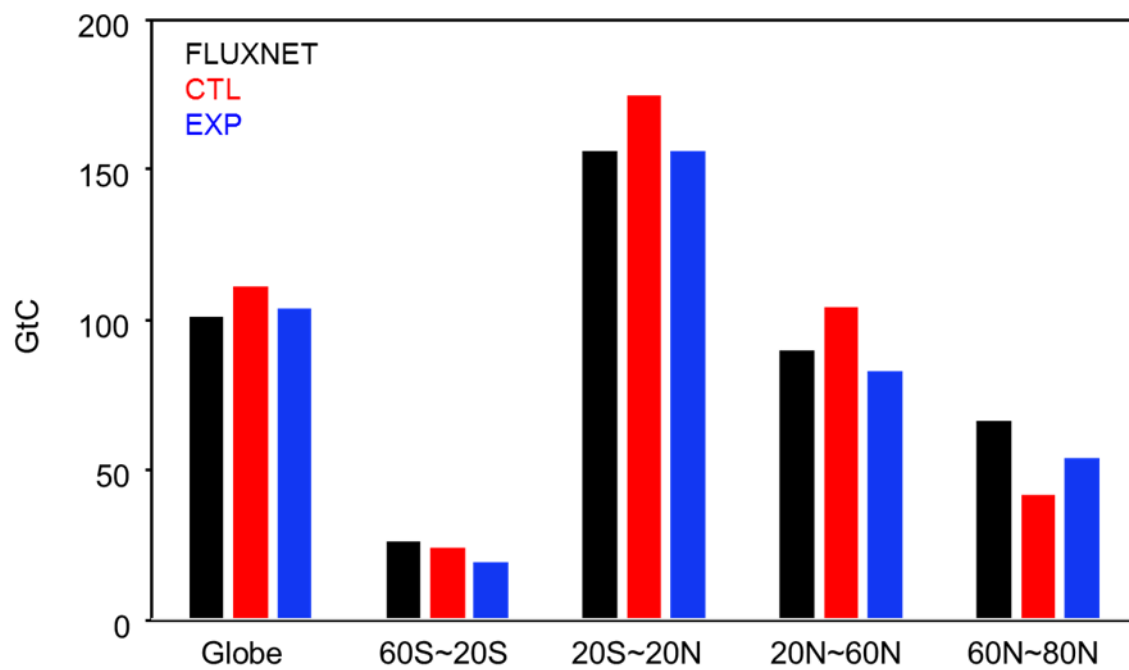


**Figure 9.** Regional averaged GPP in FLUXNET (black bars), CTL (red bars) and EXP (blue bars).



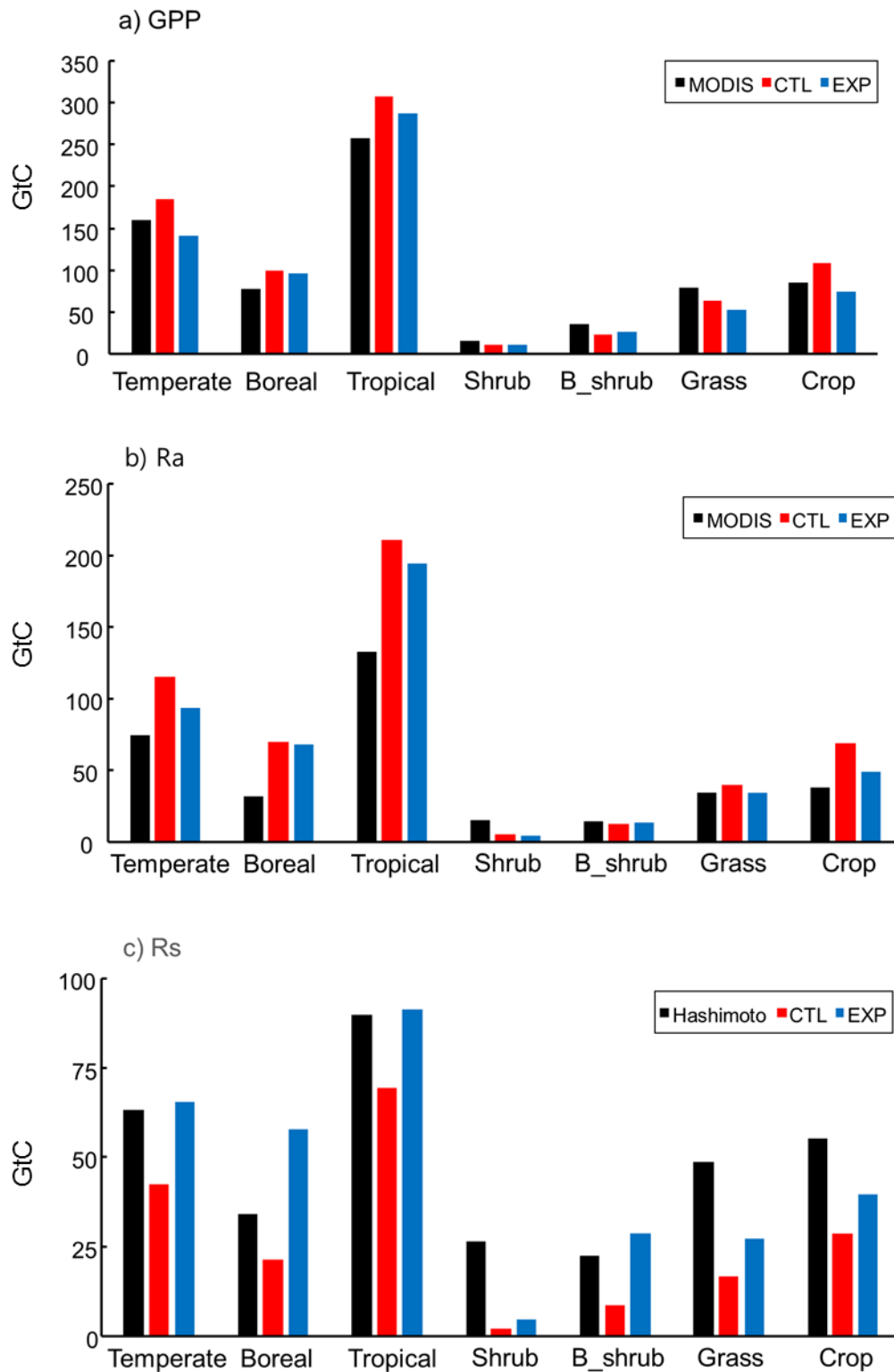


**Figure 10.** Comparison of spatial average of GPP, Ra and Rs in observation (black bars), CTL (red bars) and EXP (blue bars) by PFTs.

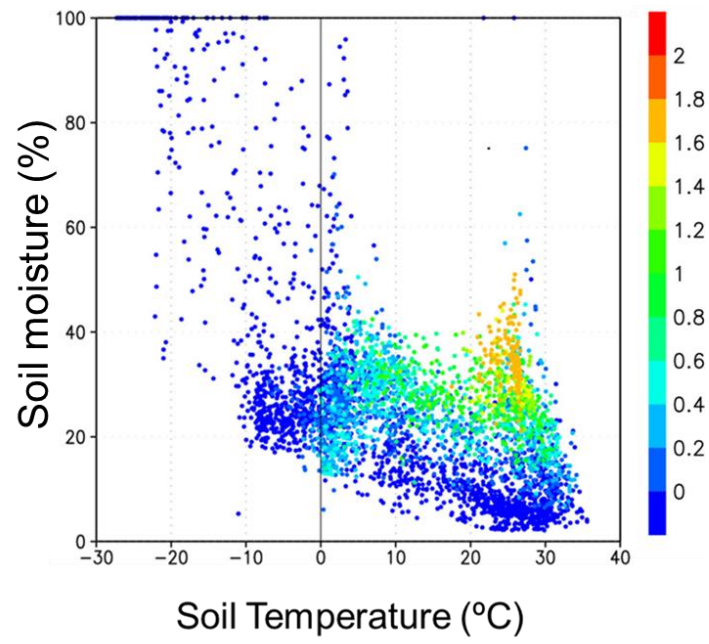


**Figure S4.** Spatial Matrix between soil moisture (Y-axis) and soil temperature (X-axis) with Rs (color dots) in the CTL simulation.